Experimental and DFT studies explain solvent control of C-H activation and product selectivity in the Rh(III)-catalysed formation of neutral and cationic heterocycles

Experimental and DFT Studies Explain Solvent Control of C-H Activation and Product Selectivity in the Rh(III)-Catalysed Formation of Neutral and Cationic Heterocycles.

David L. Davies,*,[1] Charles E. Ellul,[1] Stuart A. Macgregor,*,[2] Claire L. McMullin[2] and Kuldip Singh.[1]

[1]Department of Chemistry, University of Leicester, Leicester, LE1 7RH, UK

[2]Institute of Chemical Sciences, Heriot-Watt University, Edinburgh, EH14 4AS, UK

C-H functionalization; oxidative coupling; Rh(III); DFT; neutral and cationic heterocycles; C-N and C-C bond formation.

ABSTRACT: A range of novel heterocyclic cations have been synthesised by the Rh(III)-catalysed oxidative C–N and C–C coupling of 1-phenylpyrazole, 2-phenylpyridine and 2-vinylpyridine with alkynes (4-octyne and diphenylacetylene). The reactions proceed via initial C–H activation, alkyne insertion and reductive coupling and all three of these steps are sensitive to the substrates involved and the reaction conditions. Density functional theory (DFT) calculations show that C–H activation can proceed via a heteroatom-directed process which involves displacement of acetate by the neutral substrate to form charged intermediates. This step (which leads to cationic C–N coupled products) is therefore favored by more polar solvents. An alternative non-directed C–H activation is also possible that does not involve acetate displacement and so becomes favored in low polarity solvents, leading to C–C coupled products. Alkyne insertion is generally more favorable for diphenylacetylene over 4-octyne, but the reverse is true of the reductive coupling step. The diphenylacetylene moiety can also stabilise unsaturated 7-membered rhodacycle intermediates through extra interaction with one the Ph substituents. With 1-phenylpyrazole this effect is sufficient to suppress the final C–N reductive coupling. A comparison of a series of 7-membered rhodacycles indicates the barrier to coupling is highly sensitive to the two groups involved and follows the trend $C–N^+ > C–N > C–C$ (i.e. involving the formation of cationic C–N, neutral C–N and neutral C–C coupled products respectively).

1. Introduction

Methods to form polycyclic heterocycles through the construction of C–Y bonds (Y = C, N and O) are of vital importance for the synthesis of molecules targeting applications in pharmaceuticals and materials science. Moreover, new processes which realize this goal via the direct functionalization of C–H bonds are particularly desirable, as they avoid the pre-functionalisation of the coupling partners and so benefit from an inherently improved atom economy. Among the range of late transition metals used for such catalytic C–H functionalization, dramatic progress has been made recently in Rh-catalysed oxidative coupling, with high selectivity and functional group tolerance affording a variety of C–Y coupled products.[1] In this regard the behavior of phenylpyrazoles presents some interesting contrasts. We and others recently demonstrated that the Rh- and Ru-catalysed reactions of 3-phenylpyrazoles with internal alkynes lead to C–N coupled heterocycles (Scheme 1a).[2] However, with 1-phenylpyrazole (**1**, Scheme 1b) only C–C coupled heterocycles have been reported to date; moreover the precise outcome depends on both the nature of the alkyne and the solvent.[3] Previous studies from our groups have provided some mechanistic insight into the behavior of 1-phenylpyrazole. This species undergoes acetate-assisted C–H activation with both $[MCl_2Cp^*]_2$ (M = Rh, Ir) and $[RuCl_2(p\text{-cymene})]_2$ to form cyclometalated products (see Scheme 1(c) for the Rh complex, **2**). These can then readily (room temperature) undergo insertion of either dimethylacetylene dicarboxylate or diphenylacetylene into the M–C bond to give 7-membered rhodacycles.[4] No evidence for any subsequent C–N bond coupling to form a cationic heterocycle was seen. Indeed, it has been suggested that C–N coupling might only occur with anionic directing groups that result in neutral heterocycles.[1d] However, recently a number of groups have shown that cationic C–N coupled products can be formed with the involvement of a neutral directing group.[5] The balance between C–C bond formation (to neutral products) and C–N bond formation (to cationic products) can be subtle, with Li and coworkers highlighting the role of the nature of the carboxylate and silver salts employed.[5j] In earlier work Pfeffer *et al.* showed that alkyne insertion into cycloruthenated N,N-dimethylbenzylamine gave 7-membered heterocycles with electron withdrawing substituents on the alkyne but gave C–N coupling with electron rich alkynes.[6] Hence, the effect of a range of factors

including alkyne substituents, solvent, additives and directing group on the selectivity between C–N and C–C coupling are poorly understood.

Scheme 1. Different outcomes from the reactions of phenylpyrazoles with alkynes at Rh(III).

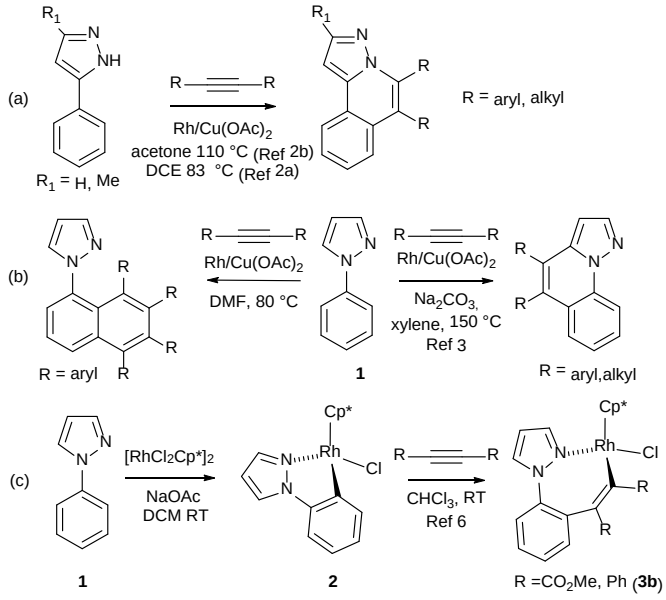

Density functional theory (DFT) calculations on C–H activation assisted by a heteroatom directing group suggest the formation of cyclometallated **2** will involve a carboxylate-assisted (AMLA/CMD) process.[7, 8] We have also highlighted the subtleties of modelling the energetics associated with the full C–H activation and functionalisation catalytic cycle.[2a, 9] Herein, we report new C–N and C–C coupling reactions of 1-phenylpyrazole, **1**, that result in the formation of cationic tricyclic and tetracyclic heterocyclic products. We also extend our study to the reactions of 2-phenylpyridine, **8**, and 2-vinylpyridine, **9**, for which only C–N coupling is observed. DFT studies provide further mechanistic insight and in combination with experiment offer a rationale for the observed product selectivities. These reaction outcomes are sensitive to the combination of the heterocyclic and alkyne substrates involved, as well as the choice of solvent and counterion. Understanding the interplay of these reaction variables is vital in the design of new catalytic processes for C–H functionalization that, as well as being efficient, must also allow control in product selectivity.

2. Experimental Studies

The different outcomes seen in the reactions of alkynes with 1-phenylpyrazole (Scheme 1b) prompted us to examine the reaction of the key C–H activated intermediate **2** with 4-octyne (**a**, Scheme 2). Remarkably, in MeOH a further new product, the cationic heterocycle **4a**, was obtained as a result of C–N coupling, in contrast to the C–C coupling processes previously reported in DMF and xylene. **4a** was obtained in quantitative yield at room temperature within 3 h, with no observable intermediates, and was fully characterised by NMR spectroscopy and by single crystal X-ray diffraction (see Supporting Information). Repeating the same reaction in chloroform gave only slow insertion of 4-octyne to form the 7-membered rhodacycle (**3a**), as observed previously with diphenylacetylene (**3b**).[4] However, redissolving **3a** in methanol led to reductive elimination and formation of **4a**. This probably reflects a greater ease of chloride dissociation in MeOH, forming a vacant site and so facilitating the reductive elimination from a 16e intermediate. Despite this, the diphenylacetylene complex **3b** showed no evidence for reductive elimination even after heating in MeOH at 60 °C for 24 h

Scheme 2. Stoichiometric reactions of C–H activated intermediate 2 with alkynes

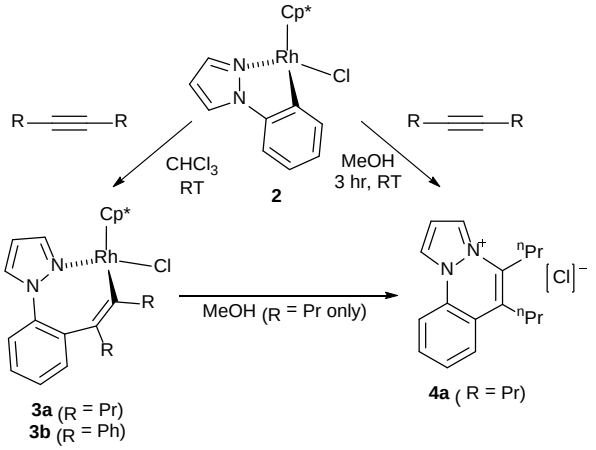

Based on these results we investigated the catalytic formation of **4a**, initially in EtOH (see Table 1). Treatment of **1** with one equivalent of 4-octyne and KPF_6, with $[RhCl_2Cp^*]_2$ (5 mol% Rh) as catalyst and $Cu(OAc)_2{\cdot}H_2O$ as oxidant, provided **4a** in 78% yield in only 1 hour (entry 1). Use of the cationic Rh precursor $[Rh(MeCN)_3Cp^*][PF_6]_2$ gave a slightly higher yield (entry 2), whilst entry 3 shows that Rh is essential. The addition of base (Na_2CO_3 or DABCO) has no significant effect (entries 4 and 5).

Table 1. Rh-Catalysed Heterocycle Formation with 1-Phenylpyrazole, **1**, and 4-octyne (**a**).

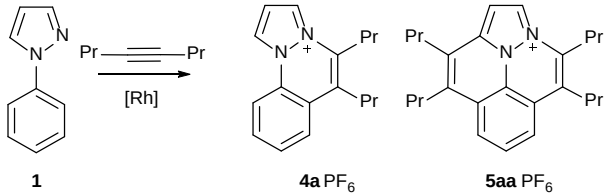

Entry	Catalyst	Solvent	Equiv Alkyne	Time (hrs)	Yield (%) 4a	5aa
1	A	EtOH	1.2	1	78	-
2	B	EtOH	1.2	1	88	-
3	None	EtOH	1.2	16	Trace	-
4[a]	B	EtOH	1.2	1	69	7
5[b]	B	EtOH	1.2	1	75	4
6	A	DCE	1.2	16	-	72[c]

7	B	DCE	2.2	1	3	58
8	B	DCE	2.2	24	-	74
9	B	EtOH	2.2	3	82	8
10	B	EtOH	2.2	24	29	57

Conditions: pyrazole (0.5 mmol): 4-octyne (see Table); Catalysts A = $[RhCl_2Cp^*]_2$ (2.5 mol%) and B = $[Rh(NCMe)_3Cp^*](PF_6)_2$ (5 mol%, *cf.* pyrazole); $Cu(OAc)_2{\cdot}H_2O$ (1.25 mmol); KPF_6 (0.6 mmol); solvent (10 mL); 83 °C; yield determined by ^{1}H NMR *vs.* 1,3,5-trimethoxybenzene (0.25 mmol). [a] Na_2CO_3 (1 mmol) [b] DABCO (0.5 mmol) [c] yield based on octyne

As with the stoichiometric experiments, solvent was again found to play a significant role in the product selectivity under catalytic conditions. Thus in DCE the major species formed was not **4a**, but the new doubly inserted product cationic **5aa**, even though the alkyne is present only in slight excess (entry 6). The identity of **5aa** was confirmed by single crystal X-ray diffraction (see Supporting Information). If the reaction was performed with 2.2 equivalents of 4-octyne (entry 7) only traces of **4a** were observed even at short reaction times, the major product being **5aa**. After 24 h only **5aa** was observed (entry 8). Repeating this reaction with 2.2 equivalents of 4-octyne in EtOH (entry 9) gave mainly **4a** (82%) after 3 h but after 24 h **5aa** was the major product (57%) along with some **4a** (29%, entry 10). In contrast the corresponding reaction of 1-phenylpyrazole with PhCCPh in EtOH gave no evidence for any cationic product of type **4** and after 24 h at 120 °C only showed low conversion (14%) to a naphthylpyrazole.

Turning to the mechanism of these processes, in EtOH it seems reasonable to postulate that **4a** is an intermediate in the formation of **5aa**. In addition, the formation of **4a** is much faster than its subsequent conversion to **5aa**. In contrast, in DCE **4a** is only observed at short reaction times and then only in small amounts, suggesting that the onward conversion of **4a** to **5aa** is faster than the initial formation of **4a** itself. Conversion of **4a** to **5aa** requires a double C–H activation without any heteroatom assistance and such processes have been reported to occur in a number of heterocycles containing acidic protons,[5j, 10] and recently for pyridinium and imidazolium salts.[11]

To investigate whether direct C–H activation of **4a** is feasible, stoichiometric cyclometallation of **4a**$[PF_6]$ with $[RhCl_2Cp^*]_2$ and NaOAc was attempted in MeOH. Monitoring by ^{1}H NMR spectroscopy showed the signals for **4a** are unchanged even after 24 h at 83 °C. Repeating the reaction in methanol-d_4 with catalytic $[RhCl_2Cp^*]_2$ led, after heating in a sealed tube at 83 °C for 48 h, to 29 % deuteration at the *ortho*-H position on the phenyl ring alongside substantial deuteration at all the pyrazole ring positions. Heating **4a**$[PF_6]$ in methanol-d_4 under the same conditions but with no Rh present also exchanged the pyrazole protons but in this case no exchange was observed at the phenyl ring. Thus the Rh-catalyst can effect the non-heteroatom directed C–H activation of **4a,** but the non-observation of any cyclometallated intermediates indicates this step is thermodynamically unfavorable, and so reversible.

To confirm that **4a** is an intermediate to **5aa**, isolated **4a**$[PF_6]$ was used as a substrate for the catalysis with 4-octyne (see Scheme 3). Surprisingly, only very low conversions to **5aa** were observed in either EtOH (3%) or DCE (8%) after 16 h. Repeating the reactions in the presence of 1 equivalent of KOAc increased the conversion of **4a** to **5aa** in both EtOH (54%) and DCE (99%). Similar results are observed in the reaction of **4a**[OAc] with 4-octyne in either DCE or EtOH, hence the presence of a significant concentration of OAc^- appears to be a key requirement to form **5aa** from **4a**. Interestingly, in contrast to 1-phenylpyrazole, **4a** will also undergo C–C coupling with diphenylacetylene in the presence of KOAc to form **5ab**.

Scheme 3. Reactions of **4a** with alkynes (X = PF_6 or OAc, see text).

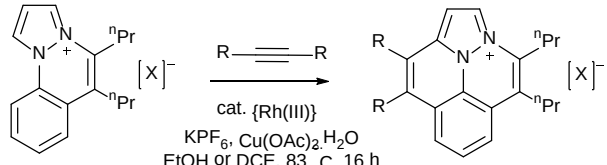

Having shown that C–N coupling to form **4a** can be followed by C–C coupling to form **5aa** and **5ab** we considered whether the reactions could be performed in the opposite order. Thus the alternative C–C coupled substrates, **6a** and **6b** were prepared using Miura's method[3b] and shown to undergo acetate-assisted cyclometallation in high yield upon treatment with $[RhCl_2Cp^*]_2$ and NaOAc (Scheme 4). Both cyclometallated complexes **7a/b** were fully characterised by NMR spectroscopy and single crystal X-ray diffraction (see Supporting Information).

Scheme 4. Cyclometallation of **6a** and **6b**.

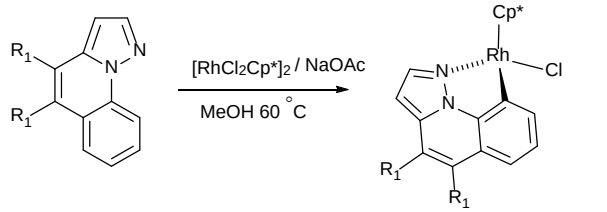

Reaction of complexes **7a/b** with 4-octyne in methanol then proceeded as for the phenylpyrazole analogue, **2** (Scheme 2) to afford cationic heterocycles **5aa** and **5ab** respectively in quantitative yield. However, in contrast to **2**, complexes **7a/b** also reacted, though more slowly, with diphenylacetylene in methanol to give cationic species **5ba** and **5bb** respectively. Hence by making the substrate more rigid the C–N coupling with diphenylacetylene will proceed. In none of these reactions was there any evidence for a 7-membered ring insertion intermediate similar to **3**.

The catalytic conversion of substrates **6** to tetracyclic cations **5** was also tested and the results are shown in Table

2. As found in the stoichiometric reactions described above, **6a** and **6b** could be catalytically converted in good yields to **5aa** and **5ab** respectively by reaction with 4-octyne. The reactions with diphenylacetylene also proceeded to give **5ba** and **5bb** respectively but in slightly reduced yields. Formation of **5bb** is least favored, giving only a 39% yield and formation of some by-products. The identity of salts **5ba** and **5bb** have both been confirmed by X-ray crystallography (see Supporting Information).

Table 2. Rh-Catalysed Coupling of 6a and 6b with Alkynes.

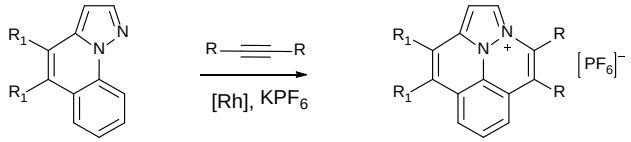

6a, R_1 = nPr
6b, R_1 = Ph

5aa, R = ^{n}Pr, R_1 = ^{n}Pr,
5ba, R = Ph, R_1 = ^{n}Pr,
5ab, R = ^{n}Pr, R_1 = Ph,
5bb, R = Ph, R_1 = Ph,

Entry	Substrate	Alkyne	Yield (%)
1	6a	4-octyne	85 (**5aa**)
2	6a	PhCCPh	52 (**5ba**)
3	6b	4-octyne	67 (**5ab**)
4	6b	PhCCPh	39 (**5bb**)

Conditions: Pyrazole (0.5 mmol), alkyne (1.2 mmol), [Rh(NCMe)3Cp*](PF6)2 (5 mol%), Cu(OAc)2·H2O (1.25 mmol), KPF6 (0.6 mmol), 1,3,5 trimethoxybenzene (0.25 mmol), EtOH (10 mL), 83 °C, yields determined by 1H NMR spectroscopy.

Having investigated the reactions of 1-phenylpyrazole we considered the effect of the heterocycle substrate on the outcome by investigating the analogous reactions with 2-phenylpyridine, **8**, and 2-vinylpyridine, **9** (Table 3). As with **1** the reactions of **8** and **9** with 4-octyne work well (Table 3, entries 1 and 3); moreover for these pyridine substrates reaction with diphenylacetylene is also successful, giving C-N coupled products in reasonable to good yield (entries 2 and 4). The same products have been recently reported using Ru or Rh catalysis.[5c, 5d, 5f] In contrast, all attempts to get the salts **10** to react further with alkynes to generate tetracyclic products (similar to the conversion of **4a** to **5aa**/**5ab**), were unsuccessful, even in DCE which was shown to promote this process for **4a**. Thus double C-H activation and C-C coupling is also highly dependent on the precise substrate employed.

Table 3. Rh-Catalysed Coupling of 2-phenylpyridine (8) and 2-vinylpyridine (9) with Alkynes.

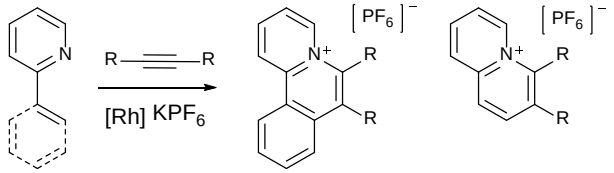

8, 2-phenylpyridine
9, 2-vinylpyridine

10a, R = nPr
10b, R = Ph

11a, R = nPr
11b, R = Ph

	Substrate	Alkyne	Product	Yield (%)
1	8	PrCCPr	10a	72
2	8	PhCCPh	10b	61
3	9	PrCCPr	11a	67
4	9	PhCCPh	11b	45

Conditions: Pyridine (0.5 mmol), alkyne (0.6 mmol), $[RhCl_2Cp^*]_2$ 2.5 mol% $Cu(OAc)_2{\cdot}H_2O$ (1.25 mmol), KPF_6 (0.6 mmol), EtOH (10 mL), 83 °C, 6 h, yield determined by ^{1}H NMR spectroscopy.

3. Computational Studies

In order to understand the factors determining the different product selectivities observed experimentally, density functional theory (DFT) calculations have been undertaken to establish the mechanisms and energetics of these various C–N and C–C oxidative coupling reactions. Experimentally, the reaction outcomes depend on the combinations of the alkyne, substrate and solvent employed. Thus with **1** in EtOH C–N coupling only occurs with 4-octyne (**a**) to give **4a**, while no equivalent C–N coupled product is seen with diphenylacetylene (**b**). In contrast, the phenyl- and vinyl-pyridines **8** and **9** react with both alkynes to form heterocycles **10a/b** and **11a/b** respectively. Tetracycle formation also depends on the system involved: the C–N strapped substrate **4a** reacts with both alkynes to form **5aa** and **5ab** and these can also be formed from the C–C strapped substrates **6a** and **6b**, from which the complementary **5ba** and **5bb** can also be accessed. In contrast, no further reaction of the C–N coupled pyridine-based heterocycles **10a/b** and **11a/b** is seen with either alkyne. The choice of solvent also affects reactivity: in EtOH the reaction of **1** to form **4a** is faster than the onward reaction of **4a** to give **5aa**. However in DCE the second C–C coupling to give tetracycle **5aa** competes with the initial C–N coupling with the result that **4a** does not build up significantly during catalysis.

In modelling these various processes with DFT calculations, all geometries have been optimised using the BP86 functional and a modest basis set (BS1). As in previous related work,[2a, 9] we report computed free energies, with corrections for solvation (PCM approach), dispersion (Grimme's D3 parameter set) and basis set effects (with a larger basis set, BS2, including diffuse functions). See the Computational Details section for full details.

Reactivity of 1 and 4a with alkynes. The free energy profiles for the initial C–H activation of 1-phenylpyrazole and the subsequent coupling with 4-octyne and diphe

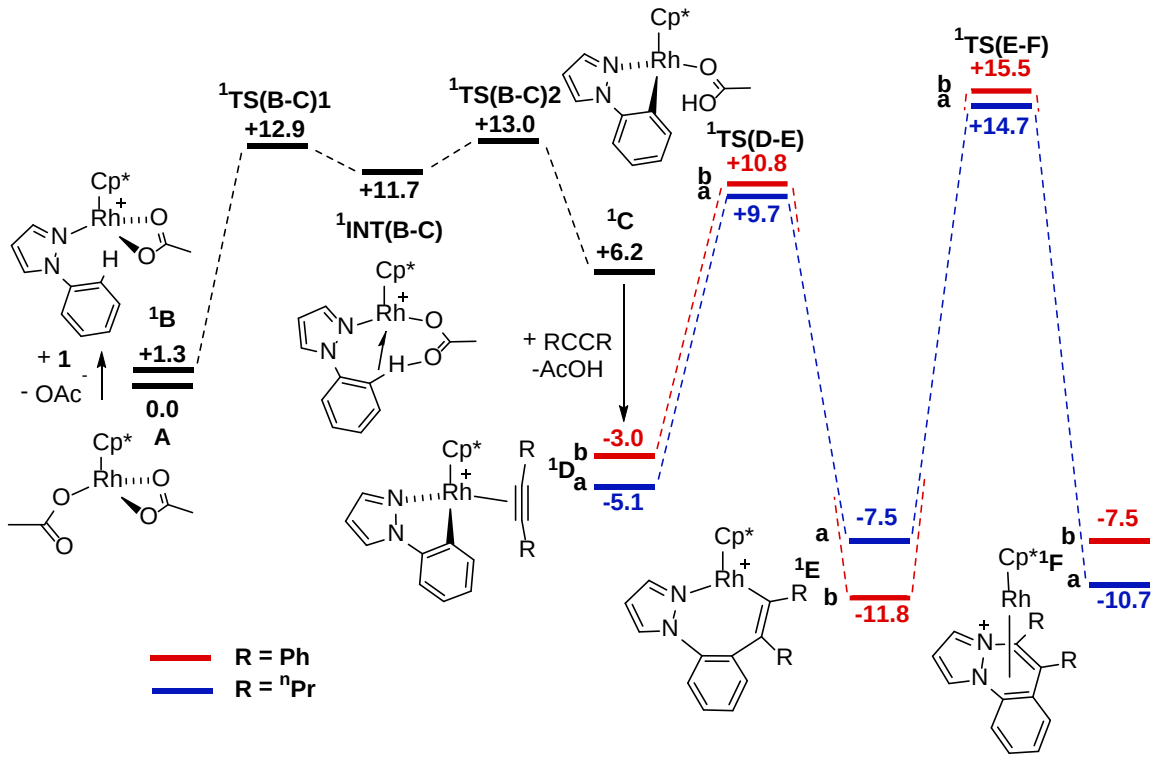

Figure 1. Computed reaction profiles (kcal/mol) for the coupling of 1-phenylpyrazole, **1**, with 4-octyne (**a**) and diphenylacetylene (**b**) at $Rh(OAc)_2Cp^*$, **A**, in EtOH. In each case free energies are quoted relative to **A** and the free substrates.

nylacetylene in EtOH are shown in Figure 1. We consider $Rh(OAc)_2Cp^*$, **A**, to be the catalytically active species formed under the reaction conditions and so all free energies are quoted relative to this species combined with those of the relevant substrates. Cyclometalation of **1** proceeds via initial substitution of an acetate ligand in **A** to give N-bound precursor **^{1}B** (G_{EtOH} = +1.3 kcal/mol, where the preceding superscript indicates the substrate involved), from which C–H activation proceeds in a formally two-step process via the agostic/H-bonded intermediate **^{1}INT(B-C)** (G_{EtOH} = +11.7). C–H activation therefore has an overall barrier of 13.0 kcal/mol and gives the cyclometallated AcOH adduct, **^{1}C**, at +6.2 kcal/mol.[12] The onward reaction with 4-octyne then involves AcOH substitution to give intermediate **^{1}Da** (G_{EtOH} = -5.1 kcal/mol) followed by sequential alkyne insertion and C–N reductive coupling to give **^{1}Fa** in which the heterocyclic product **4a** is bound to Rh in an η^4-fashion. Both these steps are exergonic and have reasonable barriers of 14.8 kcal/mol and 22.2 kcal/mol, respectively.[13]

With diphenylacetylene an analogous mechanism is computed but with some important changes in energetics. Thus intermediate **^{1}Db** is less stable than **^{1}Da** and, while the subsequent migratory insertion has a similar barrier (13.8 kcal/mol), this step becomes significantly more favorable (ΔG_{EtOH} = -8.8 kcal/mol) than with 4-octyne. This result can be traced to an additional interaction between the formally unsaturated Rh centre in **^{1}Eb** and one of the Ph substituents (Rh–C^9 = 2.31; Rh–C^{10} = 2.49 Å, see Figure 2 which also defines the atom labelling scheme employed). This greater stabilisation of **^{1}Eb** disfavors the C–N reductive coupling which has an increased barrier of 27.3 kcal/mol and becomes endergonic by 4.3 kcal/mol. These less favorable energetics are consistent with the non-observation of any heterocyclic products experimentally with diphenylacetylene, while the facile migratory insertion is in accord with the formation of the 7-membered rhodacycle, **3b**, in the stoichiometric reactions[4] (see Scheme 2). As no equivalent stabilisation occurs with the ^{n}Pr substituents in **^{1}Ea**, C–N reductive coupling from that species is both more kinetically accessible and exergonic, and can proceed to give ultimately the heterocycle **4a**. The Rh(I) species formed in this reductive coupling step can then be re-oxidised by $Cu(OAc)_2$ to regenerate catalytically active $Rh(OAc)_2Cp^*$, **A**.

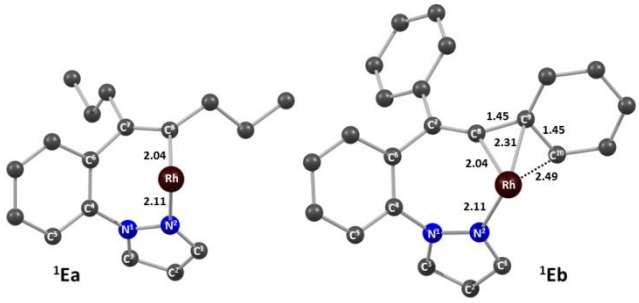

Figure 2. Computed structures of **^{1}Ea** and **^{1}Eb** with selected distances in Å. Structures are viewed approximately along the Rh–Cp* centroid axis, with the Cp* ligand and all H atoms omitted for clarity.

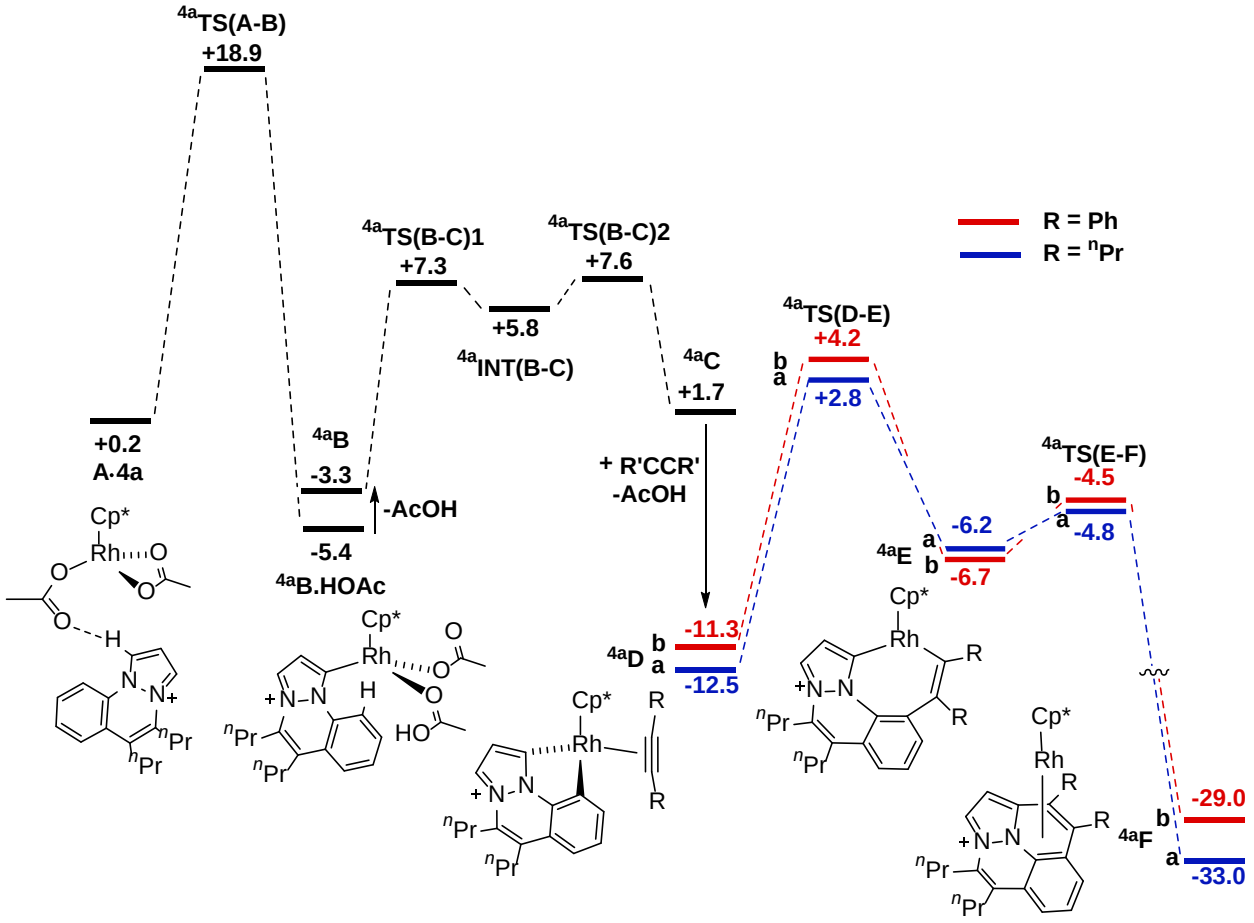

Figure 3. Computed reaction profiles (kcal/mol) for the coupling of **4a** with 4-octyne (**a**) and diphenylacetylene (**b**) at Rh(OAc)2Cp*, **A**, in EtOH. In each case free energies are quoted relative to **A** and the free substrates. The structures of ^{4a}**B**, ^{4a}**INT(B-C)** and ^{4a}**C** are analogous to ^{1}**B**, ^{1}**INT(B-C)** and ^{1}**C** in Figure 1 and so are omitted for clarity.

The onward reaction of **4a** with 4-octyne or diphenylacetylene to form tetracycles **5aa** or **5ab**, respectively, requires the double C–H bond activation of **4a** prior to the alkyne insertion and C–C reductive coupling steps. The first C–H bond activation is necessarily a non-directed process, at either the pyrazole C^3–H^3 bond or the arene C^5–H^5 bond. The former possibility was found to be more accessible and proceeds via ^{4a}**TS(A-B)** at +18.9 kcal/mol (see Figures 3 and 4), 5.0 kcal/mol below that for the alternative C^5–H^5 bond activation (see Supporting Information). The activation of the C^3–H^3 bond starts from an adduct of **A** and **4a**, **A•4a**, which displays a short contact of 1.91 Å between the protic H^3 and O^1, the pendant oxygen of the κ^1-OAc ligand. ^{4a}**TS(A-B)** then incorporates H-transfer onto oxygen ($C^3\cdots H^3$ = 1.22 Å; $O^1\cdots H^3$ = 1.59 Å) with concomitant Rh–C^3 bond formation (2.26 Å), a process that also requires the dissociation of one arm of the spectator acetate ligand to accommodate the new Rh–C bond (Rh$\cdots O^3$ = 3.44 Å *cf.* 2.20 Å in **A•4a**). After HOAc dissociation the subsequent C^5–H^5 bond activation in intermediate ^{4a}**B** (G_{EtOH} = -3.3 kcal/mol) exploits the new Rh–C^3 bond as a directing group and leads to the cyclometalated AcOH adduct ^{4a}**C** (G_{EtOH} = +1.7) through a regular two-step intramolecular acetate-assisted C–H activation. The reaction of **A** with **4a** to form ^{4a}**C** is computed to be endergonic, and to have barriers of 18.9 kcal/mol and 24.3 kcal/mol for the forward and reverse directions, respectively. This is consistent with the slow H/D exchange seen experimentally in the absence of alkyne, where relatively forcing conditions are required, as well as the non-observation of any cyclometalated intermediates.

From ^{4a}**C** the formation of **5aa** readily proceeds via substitution of AcOH by 4-octyne to give ^{4a}**Da** (G_{EtOH} = -12.5 kcal/mol) followed by insertion into the Rh–aryl bond ($\Delta G^{\ddagger}_{EtOH}$ = +15.3 kcal/mol). This step is markedly endergonic (ΔG_{EtOH} = +6.3 kcal/mol), in contrast to the equivalent step in Figure 1 (^{1}**Da** → ^{1}**Ea**, ΔG_{EtOH} = -2.4 kcal/mol) and reflects the increased rigidity imposed by the {C_2Pr_2} 'strap' in the 7-membered rhodacycle ^{4a}**Ea**. The final C–C coupling step in ^{4a}**Ea** is also far more accessible than C–N bond coupling in ^{1}**Ea**, and proceeds with a barrier of only 1.4 kcal/mol to give ^{4a}**Fa** (G_{EtOH} = -33.0 kcal/mol) in which the tetracyclic product **5aa** is bound in an η^4-fashion to Rh.

The onward reaction of ^{4a}**C** with diphenylacetylene shows very similar energetics to those computed with 4-octyne and, in particular, the final C–C bond coupling event again has a minimal barrier (2.2 kcal/mol) and is strongly

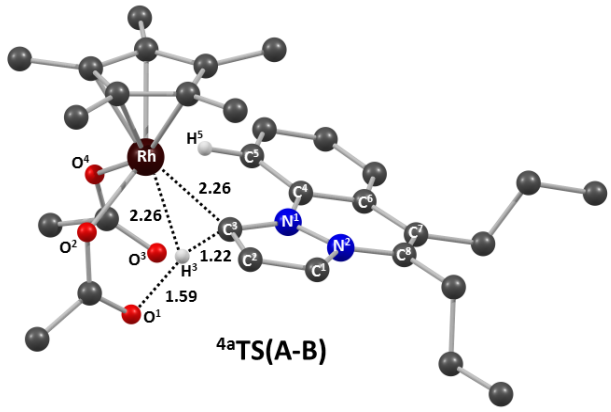

Figure 4. Computed structure of ^{4a}**TS(A-B)** with selected distances in Å. All non-participating H atoms omitted for clarity.

exergonic. **5ab** should therefore be readily formed, as is observed experimentally. The similar behavior of 4-octyne and diphenylacetylene with **4a** is in marked contrast to their reactions with **1**. This may in part reflect the intrinsically more facile C–C coupling (involving two formally anionic C-centres) that is involved in tetracycle formation compared to the C–N coupling necessary to form **4a** (combining an anionic C with a neutral N centre, see Discussion below). In addition, whereas intermediate ^{1}**Eb** was stabilised by an interaction with the alkyne phenyl substituent, no such interaction is seen in ^{4a}**Eb**, as the increased rigidity of the 'strapped' rhodacycle does not allow the substituent to approach the Rh centre (the shortest Rh···C_{phenyl} contact is to the ipso carbon, at 3.04 Å).

The marked solvent dependency of the reaction of **1** with 4-octyne prompted us to re-compute the reaction profiles in Figures 1 and 3 with a correction for DCE solvent (see Supporting Information for full details). The major change is centred on the first step in the reaction of **1** which involves the displacement of an acetate anion in **A** by the neutral substrate to form cationic **B** and free acetate. This process is more accessible in EtOH (ΔG_{EtOH} = +1.3 kcal/mol) than in DCE (ΔG_{DCE} = +5.9 kcal/mol) and has the effect of raising the overall barrier to C–H activation in DCE to +17.8 kcal/mol, compared to only 13.0 kcal/mol in EtOH. In contrast, the reaction of **4a** is less solvent dependent, as in this case it is the neutral bis-OAc species **A** that effects a non-directed C–H activation without requiring any dissociation of acetate. The energy of the key transition state in this process, ^{4a}**TS(A-B)**, is therefore not significantly affected by the solvent employed (G_{EtOH} = +18.9 kcal/mol *cf.* G_{DCE} = +18.2 kcal/mol). Under catalytic conditions once **4a** is formed it will be in competition with **1** for C–H activation at the catalytically active species **A**. In EtOH acetate loss and C–H activation of **1** ($\Delta G^{\ddagger}_{EtOH}$ = +13.0 kcal/mol) is clearly kinetically favored over the non-directed C–H activation of **4a** at **A** ($\Delta G^{\ddagger}_{EtOH}$ = +18.9 kcal/mol). Substrate **1** therefore reacts preferentially, resulting in the observed build-up of **4a** in EtOH. The onward reaction of **4a** to give **5aa** will then only occur later in the catalysis once the concentration of **1** in solution is reduced. In DCE, however, the C–H activations of both **1** and **4a** are competitive ($\Delta G^{\ddagger}_{EtOH}$ = 17.8 kcal/mol *cf.* $\Delta G^{\ddagger}_{DCE}$ = 18.2 kcal/mol) and so as **4a** is formed it can react on to give tetracycle **5aa**. A further factor in the more efficient onward reaction of **4a** in DCE is the greater stability of adduct **A**•**4a** (G_{DCE} = +0.2 kcal/mol) over intermediate ^{1}**B** (G_{DCE} = +5.9 kcal/mol) which will favor the non-directed C–H activation.[14] In contrast in EtOH these two species are much closer in energy (ΔG_{EtOH} = 1.1 kcal/mol). This difference reflects the greater propensity of acetate to dissociate in a more polar solvent and also explains the need for additional acetate to facilitate the formation of **5aa** from isolated **4a**.

Reactivity of 6a and 6b with alkynes. Experimentally the neutral C–C strapped substrates **6a** and **6b** are able to react with both 4-octyne and diphenylacetylene to form (with **6a**) tetracycles **5aa** and **5ba** and (with **6b**) **5ab** and **5bb**. Thus C–N coupling is now feasible with both alkynes, in contrast to what is observed with substrate **1**. The computed reaction profiles for the reactions of **6a** with 4-octyne and diphenylacetylene in EtOH are shown in Figure 5 (those for the reactions of **6b** are provided in the Supporting Information). The energetics of C–H activation are similar to those computed with **1**, although the more rigid structure of **6a** results in a one-step process via ^{6a}**TS(B-C)** at +14.6 kcal/mol with no agostic intermediate being located. The energetics of HOAc/alkyne substitution and migratory insertion are again similar to those computed with **1**, although, with **6a** migratory insertion is significantly endergonic for both alkynes (by *ca.* 5.5 kcal/mol) and the subsequent C–N coupling step has barriers of *ca.* 11 kcal/mol, significantly lower than from ^{1}**Ea/b**. This pattern of a thermodynamically uphill insertion followed by facile reductive coupling is similar to the behavior of the C–N strapped substrate **4a**, suggesting that the rigid strap plays an important role in promoting the reaction in both cases.

The overall barriers for C–N coupling from intermediates ^{6a}**Da** and ^{6a}**Db** are 17.4 kcal/mol and 16.1 kcal/mol respectively, consistent with both processes readily occurring experimentally. For ^{6a}**Da** the formation of the initial product ^{6a}**Fa** featuring the Rh-bound tetracycle **5aa** is exergonic by 3.3 kcal/mol, while the equivalent process with diphenylacetylene (^{6a}**Db** → ^{6a}**Fb**) is marginally uphill, and this difference may be related to the lower yield seen experimentally for **5ba** (52 %) compared to **5aa** (87 %, see Table 2). The barriers for the C–N coupling step from ^{6a}**Ea**/^{6a}**Eb** are *ca.* 10 kcal/mol higher than the equivalent C–C coupling in ^{4a}**Ea**/^{4a}**Eb**, reiterating the intrinsically greater accessibility of C–C coupling when other factors are equal. We also computed the C–H activation and coupling of substrate **6b** with 4-octyne and diphenylacetylene, to give **5ba** and **5bb**. Very similar patterns to those seen in Figure 4 were found and full details are given in the Supporting Information.

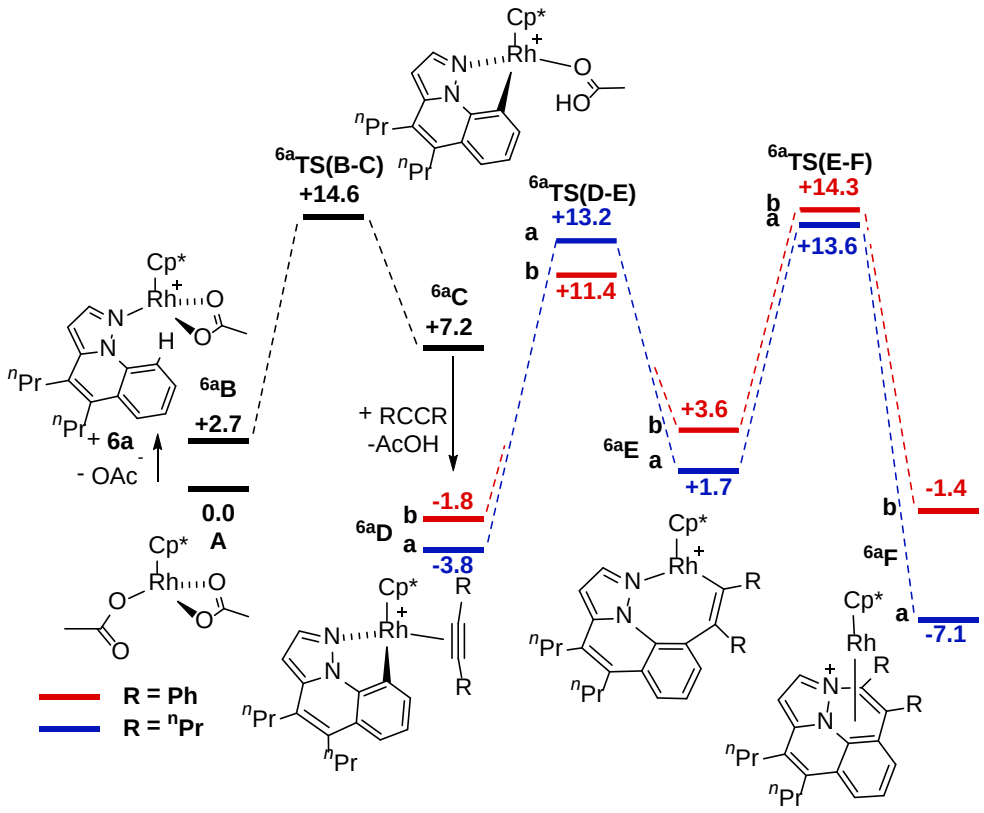

Figure 5. Computed reaction profiles (kcal/mol) for the coupling of **6a** with 4-octyne and diphenylacetylene at Rh(OAc)2Cp*, **A**. Results are computed in EtOH and free energies are quoted relative to **A** and the free substrates.

Reactions of 8 with alkynes. In contrast to the behavior seen in the reactions of **1**, **4a** and **6a**/**6b** with alkynes, 2-phenylpyridine, **8**, shows a further distinct reactivity pattern in that it undergoes C–N coupling with both 4-octyne and diphenylacetylene, but then neither of the resultant cationic heterocycles, **10a** or **10b**, reacts further to form tetracyclic products. Similar results are seen experimentally with vinylpyridine, **9**. We focus here on the computed profiles for the reactions of 2-phenylpyridine with 4-octyne and diphenylacetylene (see Figure 6, where the data are corrected for EtOH solvent). In this case substitution of OAc^- in **A** by substrate **8** followed by C–H activation proceeds a small overall barrier of only 8.8 kcal/mol to give, after HOAc/alkyne substitution, complexes ^{8}**Da** and ^{8}**Db** at -7.6 and -6.6 kcal/mol respectively. As with the 1-phenylpyrazole-based substrates, the insertion barrier is slightly lower with diphenylacetylene (12.6 kcal/mol) than with 4-octyne (15.2 kcal/mol) and this step is exergonic, as was seen with the other unstrapped substrate **1**. Importantly, the C–N reductive coupling step is also exergonic (^{8}**Ea** → ^{8}**Fa**, ΔG_{EtOH} = -7.8 kcal/mol; ^{8}**Eb** → ^{8}**Fb**, ΔG_{EtOH} = -2.5 kcal/mol) and similar barriers are now computed with both alkynes (22.8 kcal/mol from ^{8}**Ea** and 23.8 kcal/mol from ^{8}**Eb**). The computed energetics for C–N bond coupling *en route* to the formation of **10a** are therefore very similar to those computed for the reaction of **1** and 4-octyne (^{1}**Ea** → ^{1}**Fa**: ΔG_{EtOH} = -3.2 kcal/mol; $\Delta G^{\ddagger}_{EtOH}$ = 22.2 kcal/mol), while the C–N coupling to form **10b** appears to be more accessible than for **4b** (^{1}**Eb** → ^{1}**Fb**: ΔG_{EtOH} = +4.3 kcal/mol; $\Delta G^{\ddagger}_{EtOH}$ = 27.3 kcal/mol). The computed trends are therefore consistent with the observation of both **10a** and **10b** experimentally.

As with substrate **4a** the potential onward reaction of **10a** or **10b** to form tetracycles requires an initial non-directed C–H activation at **A**. This step was investigated for **10a** in EtOH and the most accessible process was found to have a barrier of 28.6 kcal/mol,[15] much higher than the barrier of 18.9 kcal/mol computed for the equivalent reaction with **4a**. C–H activation is therefore significantly harder for **10a**, so much so that onward reaction to form tetracyclic products is not observed.

4 Discussion

The current experimental and computational mechanistic studies detail the various outcomes of Rh-catalysed oxidative coupling when combining different directing group substrates (1-phenylpyrazole, 2-phenylpyridine and 2-vinylpyridine) with alkynes (4-octyne and diphenylacetylene) under varying reaction conditions (solvent and anion concentration). DFT calculations have accounted for the specific observations but also highlight some more general trends of wider relevance beyond this specific study.

Two different C–H activation processes have been characterised at $Rh(OAc)_2Cp^*$: a standard ligand directed intramolecular C–H activation and an alternative non-directed intermolecular C–H activation. For the directed C–H acti

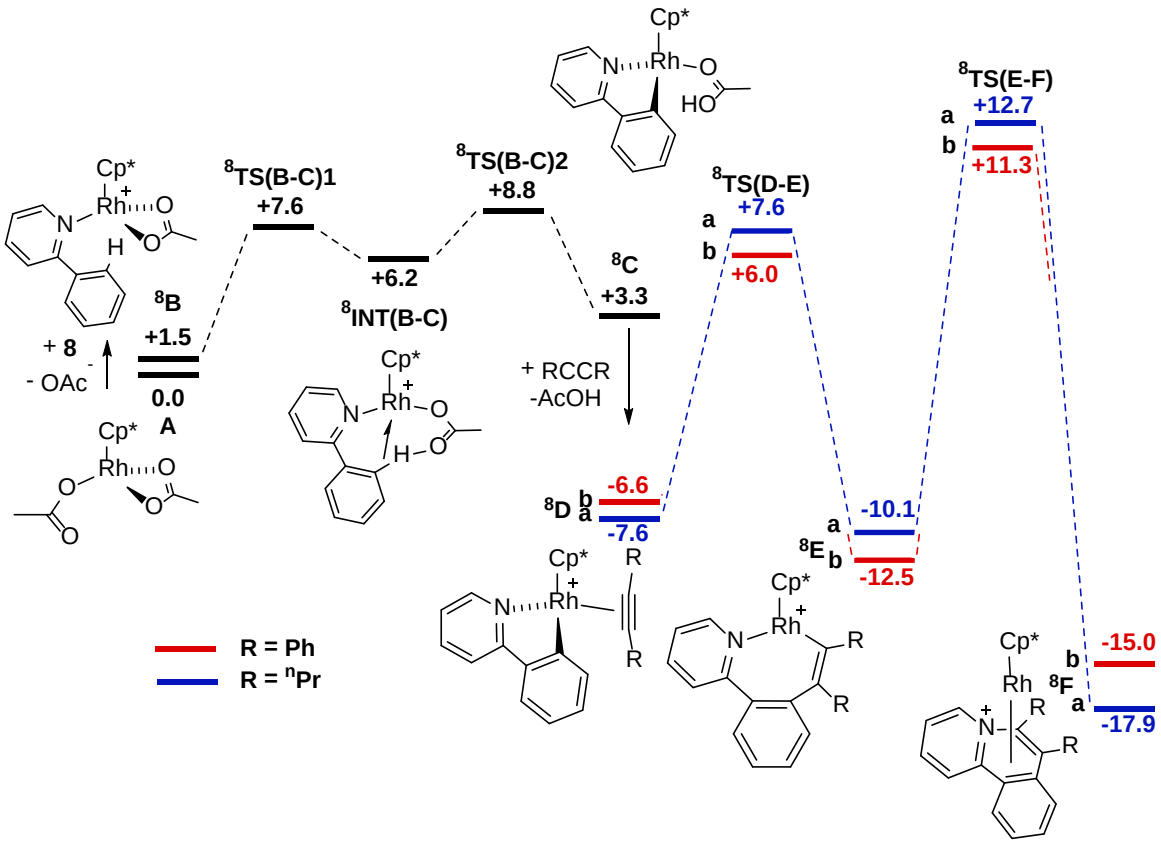

Figure 6. Computed reaction profiles (kcal/mol) for the coupling of 2-phenylpyridine, **8**, with 4-octyne and diphenylacetylene at $Rh(OAc)_2Cp^*$, **A**, in EtOH. In each case free energies are quoted relative to **A** and the free substrates.

vation the initial substitution of one acetate ligand by the directing group is required, resulting in the formation of charged intermediates that will be favored by more polar solvents. In contrast, the non-directed process necessitates both acetates to be bound to Rh and the reaction therefore proceeds through neutral intermediates, the accessibility of which will be less solvent dependent. These distinctions are confirmed in Figure 7 which displays the overall barriers computed in different solvents for both the directed and non-directed C–H activation of some of the heterocyclic substrates in this study.[16] For 1-phenylpyrazole, **1**, directed C–H activation is favored in both EtOH and DCE and alkyne insertion in these systems forms 7-membered rhodacycles that are set up for C–N bond coupling to form cationic heterocyclic products. Interestingly, the alternative non-directed C–H activation also has reasonable barriers of around 22 kcal/mol at the C^5–H^5 bond, but is actually kinetically more accessible at the backbone *ortho*-C–H bond of the phenyl group (*ca*. 19 kcal/mol). These values are also largely independent of the solvent, as anticipated. In the very low polarity xylene solvent non-directed C–H activation is favored A detailed computational study of the subsequent reaction with alkynes to give the neutral C–C coupled products reported by Miura and co-workers[3b] (*viz*. substrates **6a** and **6b** used in this study) and the observed competition for the formation of naphthalene products is currently underway.

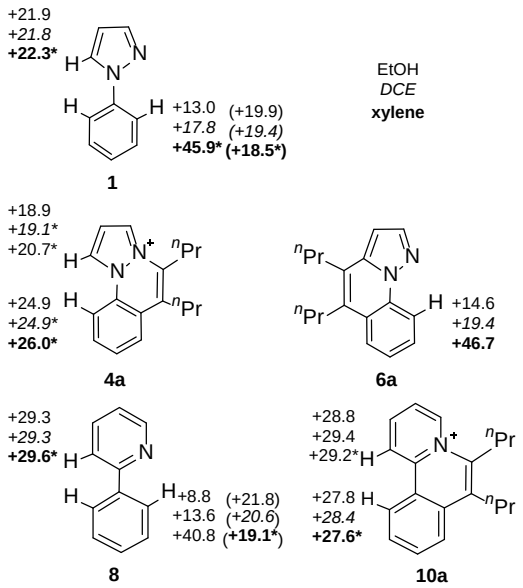

Figure 7. Computed barriers for directed and non-directed C–H activation of various heterocyclic substrates at $Rh(OAc)_2Cp^*$. Barriers are quoted relative to the most stable precursor set 0.0 kcal/mol; this is generally $Rh(OAc)_2Cp^*$ and the free substrate except in those cases marked with an asterisk where it is a H-bonded adduct (similar to **A**•**4a** in the

main text). Barriers are computed for EtOH (plain text), DCE (italics) and xylene (bold) solvents; values in parenthesis for substrates **1** and **8** are for non-directed C-H activation at the *ortho*-C-H position of the phenyl group.[12]

C–H activation barriers for the 'strapped' substrates **4a** and **6a** are also given in Figure 7. For cationic **4a** barriers for non-directed C–H activation of *ca*. 19 kcal/mol are computed in both EtOH and DCE, approximately 3 kcal/mol lower than the equivalent processes for **1**. Oxidative coupling to **5aa** and **5ab** proved possible in both solvents, although this is sensitive to the concentration of acetate (and hence the form in which this anion is introduced into the reaction) due to the need for $Rh(OAc)_2Cp^*$ to be present to effect the non-directed C–H activation. This was evident in the more efficient onward reaction of **4a** as its OAc^- rather than its PF_6^- salt. We would also predict that oxidative coupling should be possible in xylene. In contrast the directed C–H activation of **6a** is very solvent dependent: this is accessible in both EtOH and DCE leading ultimately to the formation of **5aa** and **5ba**. In xylene, however, directed C–H activation is not possible and so no further reaction to tetracyclic products is seen, as was reported by Miura. 2-phenylpyridine, **8**, has the lowest barrier to directed C–H activation of those substrates considered here, but then in contrast, isoquinolinium **10a** has the highest barriers to non-directed C–H activation, even when the slightly lower barriers at the *ortho*-C–H position are taken into account. This seems likely to relate to the lower acidity of the backbone C–H bonds associated with the pyridinium ring (with one electronegative nitrogen) compared to pyrazole-based **4a** with two nitrogens. NBO atomic charge calculations support this with a much reduced negative charge at the C^5 position in **4a** (q_C = -0.02) compared to that in **10a** (q_C = -0.22) although a similar charge of +0.28 is computed at H^5 in each case.

Comparing the two alkynes shows some subtle changes in the reaction energetics. With **1** and **8** (Figures 1 and 6) migratory insertion is always exergonic, and exhibits lower barriers and is more favorable thermodynamically for diphenylacetylene compared to 4-octyne. The opposite trend then pertains for the reductive coupling, with this difference being most apparent in the reaction with **1** where the phenyl substituent stabilises the Rh centre in the 7-membered rhodacycle, **^{1}Eb**, to such an extent that reductive coupling does not occur at all. The slightly different geometry imposed on the system by the 2-phenylpyridine moiety in **^{8}Eb** reduces this extra stabilisation and exergonic reductive coupling can still occur with an accessible barrier. With substrates **4a** and **6a** (Figures 3 and 5) the extra rigidity imposed by the backbone $\{C_2{}^nPr_2\}$ 'strap' destabilises the 7-membered rhodacycles. As a result the alkyne insertion becomes endergonic, but by the same token the final reductive coupling is facilitated; this process is again more favorable for 4-octyne compared to diphenylacetylene.

The relative reactivities of the two alkynes with **1** and **8** can also be assessed by the isodesmic reactions shown in Figure 8. The exchange of the alkyne moieties in the **4a**/**4b** and **10a**/**10b** pairs is shown to be thermodynamically uphill, indicating an intrinsic preference for the coupling reactions of 4-octyne over diphenylacetylene with both 1-phenylpyrazole and 2-phenylpyridine. It is noteworthy that this preference is slightly higher with 1-phenylpyrazole and that, experimentally, this system proved more sensitive to the alkyne identity compared to 2-phenylpyridine. Likewise exchange of the 1-phenylpyrazole and 2-phenylpyridine moieties in the **4a**/**10a** and **4b**/**10b** pairs indicates oxidative coupling is more favoured with 2-phenylpyridine, probably due to the reduced ring strain in tricyclic products featuring three 6-membered rings. The combination of 1-phenylpyrazole and diphenylacetylene is most disfavoured and this again fits with the difficulty in forming **4b** experimentally. These additional thermodynamic factors combine with the extra stabilisation of intermediate **^{1}Eb** to make the formation of **4b** inaccessible in the present system.

This and previous work allows us to monitor the ease of the final reductive coupling step as the nature of the participating groups changes. Data for five rhodacycles constructed via insertion of 4-octyne with different phenylpyrazoles are compared in Figure 9. The highest barrier ($\Delta G^{\ddagger}$ = 22.2 kcal/mol) is for the 1-phenylpyrazole system where a formally anionic alkenyl C couples with a neutral N to form a cationic heterocycle ("C-N^+ coupling"). Incorporating the $\{C_2{}^nPr_2\}$ strap reduces this barrier to 15.3 kcal/mol, for the reasons discussed above. Combining anionic C and N centres to form a neutral heterocycle (C-

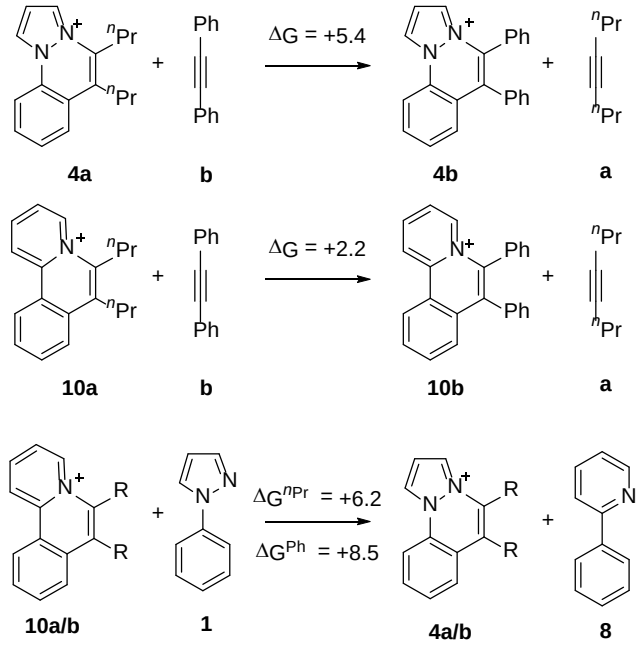

Figure 8. Calculated free energy changes (kcal/mol, in EtOH) for exchange of the alkyne moieties in **4a**/**4b** and **10**/**10b** and the 1-phenylpyrazole and 2-phenylpyridine moieties in **10a**/**4a** and **10b**/**4b**.

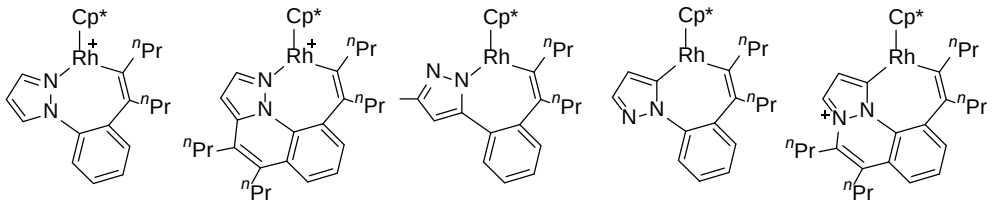

	^{1}Ea	^{6a}Ea	^{12}Ea	^{1}Ea'	^{4a}Ea
$\Delta G^{\ddagger}_{coupling}$	22.2	15.3	9.9[a]	3.9	1.4
	C-N^{+} coupling	C-N^{+} coupling	C-N coupling	C-C coupling	C-C coupling

Figure 9. Computed barriers for different C–N and C–C bond coupling processes. [a]Data from Ref 2a; see text for full details.

N coupling), as in our previous study based on 5-methyl-3-phenylpyrazole (**12**) is a much easier process, with a barrier of only 9.9 kcal/mol,[2a] less than half of that for the C–N^{+} coupling. We have also extended the current study to the coupling of two anionic C centres in **^{1}Ea'**, a species derived from **1** via non-directed C–H activation and alkyne insertion and a putative intermediate for the formation of species **6a**. Such C–C coupling is even more facile and is further facilitated (as was the case for C–N^{+} coupling) through the introduction of the {C$_2$^{n}Pr$_2$} strap as in **^{4a}Ea**.

In conclusion, we have shown through experimental and computational means how a number of steps in the Rh-catalysed oxidative coupling of N-heterocycles with alkynes can be affected by the precise substrates involved and the reaction conditions. Directed C–H activation requires substitution of acetate by the N-heterocycle and so is favored by more polar solvents. Further reaction leads to cationic tricyclic or tetracyclic products, although the ability of diphenylacetylene to stabilise a key rhodacyclic intermediate can suppress the former. Non-directed C–H activation is an energetically feasible process which, as it does not involve acetate dissociation, does not display significant solvent dependence. Hence in low polarity solvents this process becomes favored and may lead to neutral C–C coupled products. Barriers for a range of key C–Y coupling events have been assessed and shown to follow the trend C–N^{+} > C–N > C–C.

5. Experimental Section

General procedure for catalytic C,N coupling reactions Ethanol (10 mL), substrate (0.5 mmol) and alkyne (0.6 mmol), were placed into a Schlenk tube with a stirrer bar, followed by the addition of the rhodium catalyst (0.0125 mmol, 5 mol % {Rh}), KPF_6 (0.6 mmol), and $Cu(OAc)_2{\cdot}H_2O$ (1.25 mmol). The suspension was stirred at 83 °C in an oil bath. After cooling to room temperature the product was extracted into dichloromethane (2 x 10 mL) and washed with water (20 mL) containing ethylene diamine (1 mL). The organic fraction was collected and dried over $MgSO_4$. The filtrate was concentrated and the product was isolated by column chromatography using alumina eluted with ethyl acetate/methanol (100:0 to 50:50 ethyl acetate:methanol)

Computational Details. DFT calculations were run with Gaussian 03 (Revision D.01)[17] and Gaussian 09 (Revision A.02).[18] Rh centres were described with the Stuttgart RECPs and associated basis sets[19], and 6-31G** basis sets were used for all other atoms.[20] Initial BP86[21] optimizations were performed with Gaussian 03 using the 'grid=ultrafine' option, with all stationary points being fully characterized via analytical frequency calculations as either minima (all positive eigenvalues) or transition states (one negative eigenvalue). IRC calculations and subsequent geometry optimizations were used to confirm the minima linked by each transition state. All energies were recomputed with a larger basis set, BS2, featuring cc-pVTZ on Rh and 6-311++G** on all other atoms. Corrections for the effects of ethanol (ε = 24.852), dichloroethane (ε = 10.125) and xylene (ε = 2.3879) solvents were run with Gaussian 09 and used the polarizable continuum model.[22] Single-point dispersion corrections to the BP86 results employed Grimme's D3 parameter set as implemented in Gaussian 09.[23]

ASSOCIATED CONTENT

Crystallographic data (CIF), full experimental details, NMR spectra, details of kinetics and KIE measurements, and details of all computed structures and associated energies, as well as functional testing. This material is available free of charge via the Internet at http://pubs.acs.org. CCDC 1062469-1062474 contain complete crystallographic data for this paper. These data can be obtained free of charge from The Cambridge Crystallographic Data Centre via www.ccdc.cam.ac.uk/data_ request/cif.

AUTHOR INFORMATION

Corresponding Author

*E-mail: dld3@le.ac.uk. *E-mail: s.a.macgregor@hw.ac.uk.

Notes

The authors declare no competing financial interest.

Acknowledgements

This work was supported through EPSRC awards EP/J021709/1, EP/J002917/1 (D.L.D., C.E.E.), and EP/J021911/1 (S.A.M., C.L.M.). We also thank Johnson Matthey for a loan of rhodium trichloride.

REFERENCES

1. (a) Satoh, T.; Miura, M., *Chem. -Eur. J.* **2010,** *16*, 11212-11222; (b) Colby, D. A.; Tsai, A. S.; Bergman, R. G.; Ellman, J. A., *Acc. Chem. Res.* **2011,** *45*, 814-825; (c) Colby, D. A.; Bergman, R. G.; Ellman, J. A., *Chem. Rev.* **2009,** *110*, 624-655; (d) Song, G.; Wang, F.; Li, X., *Chem. Soc. Rev.* **2012,** *41*, 3651-3678; (e) Song, G.; Li, X., *Acc. Chem. Res.* **2015,** *48*, 1007-1020; (f) Patureau, F. W.; Wencel-Delord, J.; Glorius, F., *Aldrichimica Acta* **2012,** *45*, 31-41.

2. (a) Algarra, A. G.; Cross, W. B.; Davies, D. L.; Khamker, Q.; Macgregor, S. A.; McMullin, C. L.; Singh, K., *J. Org. Chem.* **2014,** *79*, 1954-1970; (b) Li, X.; Zhao, M., *J. Org. Chem.* **2011,** *76*, 8530-8536; (c) Ma, W.; Graczyk, K.; Ackermann, L., *Org. Lett.* **2012,** *14*, 6318-6321.

3. (a) Umeda, N.; Tsurugi, H.; Satoh, T.; Miura, M., *Angew. Chem. Int. Ed.* **2008,** *47*, 4019-4022; (b) Umeda, N.; Hirano, K.; Satoh, T.; Shibata, N.; Sato, H.; Miura, M., *J. Org. Chem.* **2010,** *76*, 13-24.

4. Boutadla, Y.; Davies, D. L.; Al-Duaij, O.; Fawcett, J.; Jones, R. C.; Singh, K., *Dalton Trans.* **2010,** *39*, 10447-10457.

5. (a) Li, L.; Brennessel, W. W.; Jones, W. D., *J. Am. Chem. Soc.* **2008,** *130*, 12414-12419; (b) Zhang, G.; Yang, L.; Wang, Y.; Xie, Y.; Huang, H., *J. Am. Chem. Soc.* **2013,** *135*, 8850-8853; (c) Luo, C.-Z.; Gandeepan, P.; Jayakumar, J.; Parthasarathy, K.; Chang, Y.-W.; Cheng, C.-H., *Chem. -Eur. J.* **2013,** *19*, 14181-14186; (d) Luo, C.-Z.; Gandeepan, P.; Cheng, C.-H., *Chem. Commun.* **2013,** *49*, 8528-8530; (e) Senthilkumar, N.; Gandeepan, P.; Jayakumar, J.; Cheng, C.-H., *Chem. Commun.* **2014,** *50*, 3106-3108; (f) Luo, C.-Z.; Jayakumar, J.; Gandeepan, P.; Wu, Y.-C.; Cheng, C.-H., *Org. Lett.* **2015,** *17*, 924-927; (g) Muralirajan, K.; Cheng, C.-H., *Chem. -Eur. J.* **2013,** *19*, 6198-6202; (h) Jayakumar, J.; Parthasarathy, K.; Cheng, C.-H., *Angew. Chem., Int. Ed.* **2012,** *51*, 197-200; (i) Zhao, D.; Wu, Q.; Huang, X.; Song, F.; Lv, T.; You, J., *Chem. -Eur. J.* **2013,** *19*, 6239-6244; (j) Qi, Z.; Yu, S.; Li, X., *J. Org. Chem.* **2015,** *80*, 3471-3479.

6.(a) Pfeffer, M.; Sutter, J. P.; Urriolabeitia, E. P., *Bull. Soc. Chim . Fr.* **1997,** *134*, 947-954; (b) Abbenhuis, H. C. L.; Pfeffer, M.; Sutter, J.-P.; de Cian, A.; Fischer, J.; Ji, H. L.; Nelson, J. H., *Organometallics* **1993,** *12*, 4464-4472.

7. (a) Boutadla, Y.; Davies, D. L.; Macgregor, S. A.; Poblador-Bahamonde, A. I., *Dalton Trans.* **2009**, 5887-5893; (b) Davies, D. L.; Donald, S. M. A.; Al-Duaij, O.; Fawcett, J.; Little, C.; Macgregor, S. A., *Organometallics* **2006,** *25*, 5976-5978; (c) Davies, D. L.; Donald, S. M. A.; Al-Duaij, O.; Macgregor, S. A.; Pölleth, M., *J. Am. Chem. Soc.* **2006,** *128*, 4210-4211; (d) Davies, D. L.; Donald, S. M. A.; Macgregor, S. A., *J. Am. Chem. Soc.* **2005,** *127*, 13754-13755; (e) Guimond, N.; Gorelsky, S. I.; Fagnou, K., *J. Am. Chem. Soc.* **2011,** *133*, 6449-6457; (f) Lapointe, D.; Fagnou, K., *Chem. Lett.* **2010,** *39*, 1119-1126.

8. For recent exampoles ar Rh(III) see: (a) Wu, S.; Zeng, R.; Fu, C.; Yu, Y.; Zhang, X.; Ma, S., *Chem. Sci.* **2015,** *6*, 2275-2285; (b) Wu, J.-Q.; Qiu, Z.-P.; Zhang, S.-S.; Liu, J.-G.; Lao, Y.-X.; Gu, L.-Q.; Huang, Z.-S.; Li, J.; Wang, H., *Chem. Commun.* **2015,** *51*, 77-80; (c) Chen, W.-J.; Lin, Z., *Organometallics* **2015,** *34*, 309-318; (d) Li, J.; Hu, W.; Peng, Y.; Zhang, Y.; Li, J.; Zheng, W., *Organometallics* **2014,** *33*, 2150-2159.

9. (a) Algarra, A. G.; Davies, D. L.; Khamker, Q.; Macgregor, S. A.; McMullin, C. L.; Singh, K.; Villa-Marcos, B., *Chem. -Eur. J.* **2015,** *21*, 3087-3096; (b) Carr, K. J. T.; Davies, D. L.; Macgregor, S. A.; Singh, K.; Villa-Marcos, B., *Chem. Sci.* **2014,** *5*, 2340-2346.

10. (a) Dong, L.; Huang, J.-R.; Qu, C.-H.; Zhang, Q.-R.; Zhang, W.; Han, B.; Peng, C., *Org. Biomol. Chem.* **2013,** *11*, 6142-6149; (b) Huang, J.-R.; Zhang, Q.-R.; Qu, C.-H.; Sun, X.-H.; Dong, L.; Chen, Y.-C., *Org. Lett.* **2013,** *15*, 1878-1881; (c) Lewis, J. C.; Bergman, R. G.; Ellman, J. A., *Acc. Chem. Res.* **2008,** *41*, 1013-1025.

11. (a) Cross, W. B.; Razak, S.; Singh, K.; Warner, A. J., *Chem. -Eur. J.* **2014,** *20*, 13203-13209; (b) Ghorai, D.; Choudhury, J., *ACS Catal.* **2015,** *5*, 2692-2696; (c) Ghorai, D.; Choudhury, J., *Chem. Commun.* **2014,** *50*, 15159-15162.

12. An alternative transition state for deprotonation by an external acetate was also characterised and found to be less accessible (G_{EtOH} = +23.3 kcal/mol). Competing external deprotonation was considered for all directed C-H activation processes and was always found to be less accessible.

13. The alternative alkyne insertions into the Rh–N bonds of ^{i}**Da/b** are considerably harder, with transition states approximately 19 kcal/mol above ^{i}**TS(D-E)a/b**.

14. In the absence of a second OAc C–H activation of **4a** at cationic $[Rh(OAc)Cp^*]^+$ proceeds via a transition state at +34.3 kcal/mol. An external base mechanism was more competitive in this case and involves a transiton state at +20.8 kcal/mol.

15. Non-directed C-H activation at the *ortho*-C-H bond of the phenyl group is in fact slightly more favourable in this case, although the barrier in EtOH remains high at 27. 8 kcal/mol. See Discussion section.

16. For related computational studies of non-directed C-H bond activation at Pd see: (a) Gorelsky, S. I.; Lapointe, D.; Fagnou, K., J. Org. Chem. **2012**, *77*, 658-668; (b) Petit, A.; Flygare, J.; Miller, A. T.; Winkel, G.; Ess, D. H., *Org. Lett.* **2012,** *14*, 3680-3683

17. Gaussian 03 (Revision D.01); Frisch, M. J.; Trucks, G. W.; Schlegel, H. B.; Scuseria, G. E.; Robb, M. A.; Cheeseman, J. R.; Montgomery, Jr., J. A.; Vreven, T.; Kudin, K. N.; Burant, J. C.; Millam, J. M.; Iyengar, S. S.; Tomasi, J.; Barone, V.; Mennucci, B.; Cossi, M.; Scalmani, G.; Rega, N.; Petersson, G. A.; Nakatsuji, H.; Hada, M.; Ehara, M.; Toyota, K.; Fukuda, R.; Hasegawa, J.; Ishida, M.; Nakajima, T.; Honda, Y.; Kitao, O.; Nakai, H.; Klene, M.; Li, X.; Knox, J. E.; Hratchian, H. P.; Cross, J. B.; Bakken, V.; Adamo, C.; Jaramillo, J.; Gomperts, R.; Stratmann, R. E.; Yazyev, O.; Austin, A. J.; Cammi, R.; Pomelli, C.; Ochterski, J. W.; Ayala, P. Y.; Morokuma, K.; Voth, G. A.; Salvador, P.; Dannenberg, J. J.; Zakrzewski, V. G.; Dapprich, S.; Daniels, A. D.; Strain, M. C.; Farkas, O.; Malick, D. K.; Rabuck, A. D.; Raghavachari, K.; Foresman, J. B.; Ortiz, J. V.; Cui, Q.; Baboul, A. G.; Clifford, S.; Cioslowski, J.; Stefanov, B. B.; Liu, G.; Liashenko, A.; Piskorz, P.; Komaromi, I.; Martin, R. L.; Fox, D. J.; Keith, T.; Al-Laham, M. A.; Peng, C. Y.; Nanayakkara, A.; Challacombe, M.; Gill, P. M. W.; Johnson, B.; Chen, W.; Wong, M. W.; Gonzalez, C.; and Pople, J. A.; Gaussian, Inc., Wallingford CT, 2004.

18. Gaussian 09 (Revision D.01); Frisch, M. J.; Trucks, G. W.; Schlegel, H. B.; Scuseria, G. E.; Robb, M. A.; Cheeseman, J. R.; Scalmani, G.; Barone, V.; Mennucci, B.; Petersson, G. A.; Nakatsuji, H.; Caricato, M.; Li, X.; Hratchian, H. P.; Izmaylov, A. F.; Bloino, J.; Zheng, G.; Sonnenberg, J. L.; Hada, M.; Ehara, M.; Toyota, K.; Fukuda, R.; Hasegawa, J.; Ishida, M.; Nakajima, T.; Honda, Y.; Kitao, O.; Nakai, H.; Vreven, T.; J. A. Montgomery, J.; Peralta, J. E.; Ogliaro, F.; Bearpark, M.; Heyd, J. J.; Brothers, E.; Kudin, K. N.; Staroverov, V. N.; Kobayashi, R.; Normand, J.; Raghavachari, K.; Rendell, A.; Burant, J. C.; Iyengar, S. S.; Tomasi, J.; Cossi, M.; Rega, N.; Millam, J. M.; Klene, M.; Knox, J. E.; Cross, J. B.; Bakken, V.; Adamo, C.; Jaramillo, J.; Gomperts, R.; Stratmann, R. E.; Yazyev, O.; Austin, A. J.; Cammi, R.; Pomelli, C.; Ochterski, J. W.; Martin, R. L.; Morokuma, K.; Zakrzewski, V. G.; Voth, G. A.; Salvador, P.; Dannenberg, J. J.; Dapprich, S.; Daniels, A. D.; Farkas, O.; Foresman, J. B.; Ortiz, J. V.; Cioslowski, J.; Fox, D. J.; Gaussian Inc., Wallingford, CT, 2009.

19. Andrae, D.; Häußermann, U.; Dolg, M.; Stoll, H.; Preuß, H., *Theor. Chim. Acta* **1990,** *77*, 123-141.

20. (a) Hariharan, P. C.; Pople, J. A., *Theor. Chim. Acta* **1973,** *28*, 213-222; (b) Hehre, W. J.; Ditchfield, R.; Pople, J. A., *J. Chem. Phys.* **1972,** *56*, 2257-&.

21. (a) Becke, A. D., *Phys. Rev. A* **1988,** *38*, 3098; (b) Perdew, J. P., *Phys. Rev. B* **1986,** *33*, 8822-8824.
22. Tomasi, J.; Mennucci, B.; Cammi, R., *Chem. Rev.* **2005,** *105*, 2999-3094.
23. Grimme, S.; Antony, J.; Ehrlich, S.; Krieg, H., *J. Chem. Phys.* **2010,** *132*, 154104.
.

Authors are required to submit a graphic entry for the Table of Contents (TOC) that, in conjunction with the manuscript title, should give the reader a representative idea of one of the following: A key structure, reaction, equation, concept, or theorem, etc., that is discussed in the manuscript. Consult the journal's Instructions for Authors for TOC graphic specifications.

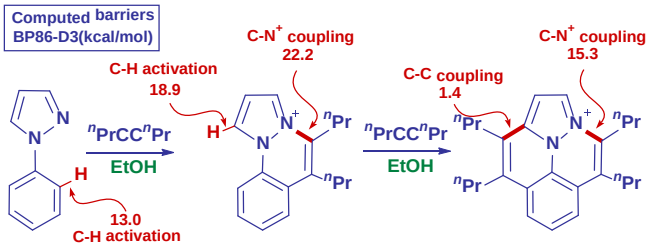

Insert Table of Contents artwork here